





Article

Application of Three Metaheuristic Techniques in Simulation of Concrete Slump

Hossein Moayed ^{1,2,*} , Bahareh Kalantar ³ , Loke Kok Foong ^{4,*} , Dieu Tien Bui ⁵  and Alireza Motevalli ⁶

¹ Department for Management of Science and Technology Development, Ton Duc Thang University, Ho Chi Minh City, Vietnam

² Faculty of Civil Engineering, Ton Duc Thang University, Ho Chi Minh City, Vietnam

³ RIKEN Center for Advanced Intelligence Project, Goal-Oriented Technology Research Group, Disaster Resilience Science Team, Tokyo 103-0027, Japan; Bahareh.kalantar@riken.jp

⁴ Institute of Research and Development, Duy Tan University, Da Nang 550000, Viet Nam

⁵ Geographic Information System Group, Department of Business and IT, University of South-Eastern Norway, N-3800 Bø i Telemark, Norway; dieu.t.bui@usn.no

⁶ Department of Watershed Management Engineering, College of Natural Resources and Marine Sciences, Tarbiat Modares University, Noor 46414-356, Iran; ar.motevalli@modares.ac.ir

* Correspondence: hossein.moayed@tdtu.edu.vn (H.M.); lokekokofoong@duytan.edu.vn (L.K.F.)

Received: 28 August 2019; Accepted: 24 September 2019; Published: 16 October 2019



Abstract: Slump is a workability-related characteristic of concrete mixture. This paper investigates the efficiency of a novel optimizer, namely ant lion optimization (ALO), for fine-tuning of a neural network (NN) in the field of concrete slump prediction. Two well-known optimization techniques, biogeography-based optimization (BBO) and grasshopper optimization algorithm (GOA), are also considered as benchmark models to be compared with ALO. Considering seven slump effective factors, namely cement, slag, water, fly ash, superplasticizer (SP), fine aggregate (FA), and coarse aggregate (CA), the mentioned algorithms are synthesized with a neural network to determine the best-fitted neural parameters. The most appropriate complexity of each ensemble is also found by a population-based sensitivity analysis. The findings revealed that the proposed ALO-NN model acquires a good approximation of concrete slump, regarding the calculated root mean square error (RMSE = 3.7788) and mean absolute error (MAE = 3.0286). It also outperformed both BBO-NN (RMSE = 4.1859 and MAE = 3.3465) and GOA-NN (RMSE = 4.9553 and MAE = 3.8576) ensembles.

Keywords: concrete; slump; neural computing; ant lion optimizer

1. Introduction

As a fundamental material in almost every civil engineering activity, concrete is a widely-used man-made mixture, composed of some basic elements (like cement and water) and additional materials. Other than the reasonable compressive strength of concrete, flowability is another determinant factor which helps workers to form concrete into any desired shape [1]. Up to now, considering the various properties of concrete (e.g., durability and early age strength), different versions of this material (e.g., ready mix (RM) and self-compacting concretes) have been produced. Out of those, high performance concrete (HPC) is special; it is famous for its workability, which is mainly influenced by the ratio of finer particles [2]. Slump is a determinant factor of concrete which directly contributes to the workability of a mixture [3]. Hence, producing a mixture with a proper slump is significant. On the other hand, there are various parameters like cement/water ratio that considerably affect the slump. Therefore, indirect measurement of slump has received growing attention for analyzing the effect of these ingredients. Among the diverse methods suggested for evaluating and predicting slump, intelligent models like

artificial neural networks (ANNs) have shown promise. ANNs are capable predictive tools that mimic the biological neural systems [4–8]. The main advantage of this model in comparison with traditional predictive models (like linear regression) lies in the capability of analyzing the non-linear relationship between independent and dependent variables (slump and effective factors in the present work) [9], which has driven many scholars to employ it for various engineering issues [10–13]. More specifically, the network tries to adjust the computational parameters pertaining to effective factors through a back-propagation procedure. In this method, the error of the performance is calculated and then, is considered in a back-ward path. This process leads to setting more compatible parameters of a network [14–18]. Different intelligent models have been used to investigate various characteristics of concrete [19–22]. In the case of ANNs, Öztaş et al. [23] successfully used this tool for predicting the slump and compressive strength of high strength concrete. Yeh [24] investigated the effect of slump influential factors, including superplasticizer-binder ratio (SP/B), water/binder ratio (w/b), and water content using ANNs. Yeh [25] developed an ANN-based methodology for simulating the slump of fly ash and slag concrete (FSC). Additionally, the relationship between the slump and concrete component was examined by response trace plots.

Moreover, a number of researchers have used hybrid evolutionary algorithms in different fields [26–29]. For slump modelling, Xu et al. [30] established a geometric semantic genetic programming (GSGP) for predicting recycled concrete slump. Chandwani et al. [31] coupled ANN with a genetic algorithm (GA) for estimating the slump of RM concrete. With respect to the obtained root mean square errors (RMSEs) of 3.4634 and 2.4994, as well as regressions of 0.9605 and 0.9791, respectively, for the typical ANN and GA-ANN models, they concluded that the proposed hybrid model was suitable for the purpose of slump prediction. Likewise, Chen et al. [32] used a parallel hyper-cubic gene expression programming (GEP) for estimating the slump flow of HPC concrete. Their findings showed that the proposed hybrid model outperformed typical GEP approach. As stated above, despite the wide application of typical predictive methods for slump prediction issues, few studies have conducted optimization of these networks using metaheuristic approaches. Hence, the focal objective of this paper is to present a novel optimization of an ANN, namely ant lion optimization (ALO), used for fine-tuning the computational parameters in concrete slump simulation.

2. Methodology

The steps taken for fulfilling the objective of this research are depicted in Figure 1. According to this figure, after providing the required data, the proposed ALO, as well as the benchmark methods of biogeography-based optimization (BBO) and the grasshopper optimization algorithm (GOA), were mathematically coupled with a typical NN using the programming language of MATLAB 2014. The best complexity of each ensemble is then determined by testing different population sizes for each network. The results of the elite structures are then evaluated by two broadly used error criteria, namely root mean square error (RMSE) and mean absolute error (MAE). The formulation of these criteria is explained below:

$$MAE = \frac{1}{N} \sum_{i=1}^N |Y_{i_{observed}} - Y_{i_{predicted}}| \quad (1)$$

$$RMSE = \sqrt{\frac{1}{N} \sum_{i=1}^N [(Y_{i_{observed}} - Y_{i_{predicted}})]^2} \quad (2)$$

in which N is the number of samples, $Y_{i_{observed}}$ and $Y_{i_{predicted}}$ denote the actual and predicted slump values.

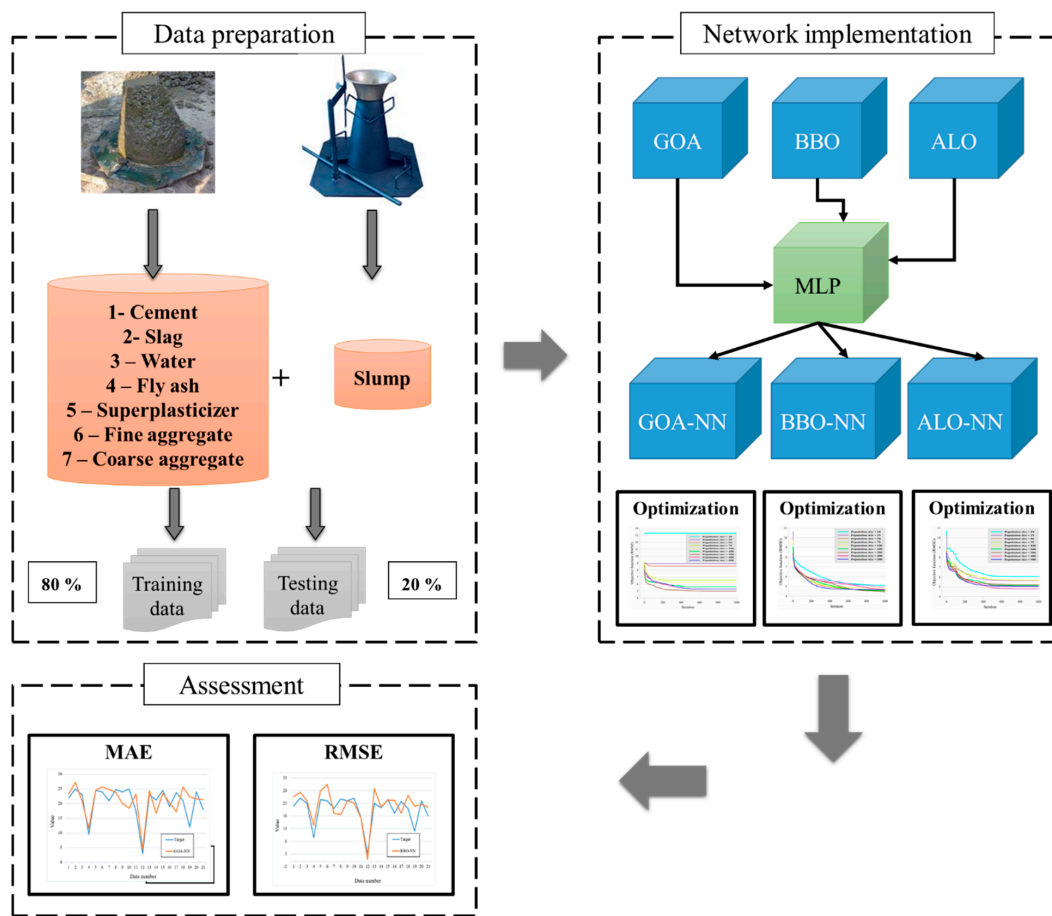


Figure 1. The graphical methodology of the present ant lion optimization (ALO)-based study.

The used methods are described in the following:

2.1. Ant Lion Optimization

As a novel swarm-based optimization technique, Mirjalili [33] introduced ant lion optimization (ALO) by mimicking the behavior of ant lions during their larvae life cycle. Similar to any optimization method, ALO aims to find the most fitted solution for a problem within a number of iterations. Initial positions of the ant lion and the prey are stochastically set within the search space. Figure 2 shows the flowchart of this algorithm. Six operations that are implemented in each iteration are (i) random walk of prey; (ii) trapping in holes; (iii) constructing a trap; (iv) sliding of prey towards the ant lion; (v) catching the prey/reconstructing the hole; and (vi) determining the elite ant lion [33,34].

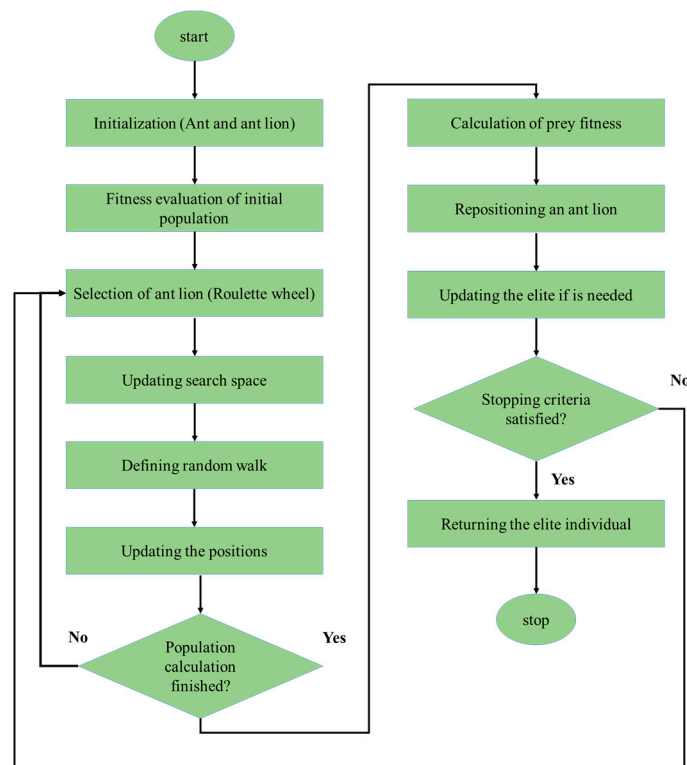


Figure 2. The flowchart of the ALO algorithm.

As Equation (3) expresses, the movement of the considered prey in this algorithm (i.e., ants) is expressed with a cumulative sum (Csum) function:

$$X(t) = [0, Csum (2r(t_1)) - 1, \dots, Csum (2r(t_n)) - 1] \tag{3}$$

$$r(t) = \begin{cases} 1, & rand(0, 1) > 0.5 \\ 0, & rand(0, 1) \leq 0.5 \end{cases} \tag{4}$$

where *rand* stands for a random number which is uniformly distributed in the interval of [0,1].

Then, assuming X_i^t as the position of the i^{th} variable in the t^{th} iteration, a normalization function is applied at each iteration as follows:

$$X_i^t = \frac{(X_i^t - a_i) \cdot (d_i^t - c_i^t)}{b_i - a_i} + c_i^t \tag{5}$$

where d_i^t and c_i^t define the maximum and minimum of the proposed variable, b_i and a_i are maximum and minimum of random walk in the i^{th} variable.

Equations (6) and (7) describe the mathematical effect of the ant lion’s holes on the prey random walk (Figure 3a):

$$c_i^t = Antlion_j^t + c^t \tag{6}$$

$$d_i^t = Antlion_j^t + d^t \tag{7}$$

in which $Antlion_j^t$ is the position of j^{th} ant lion. In addition, d^t and c^t symbolize the vectors including the maximum and minimum of all variables.

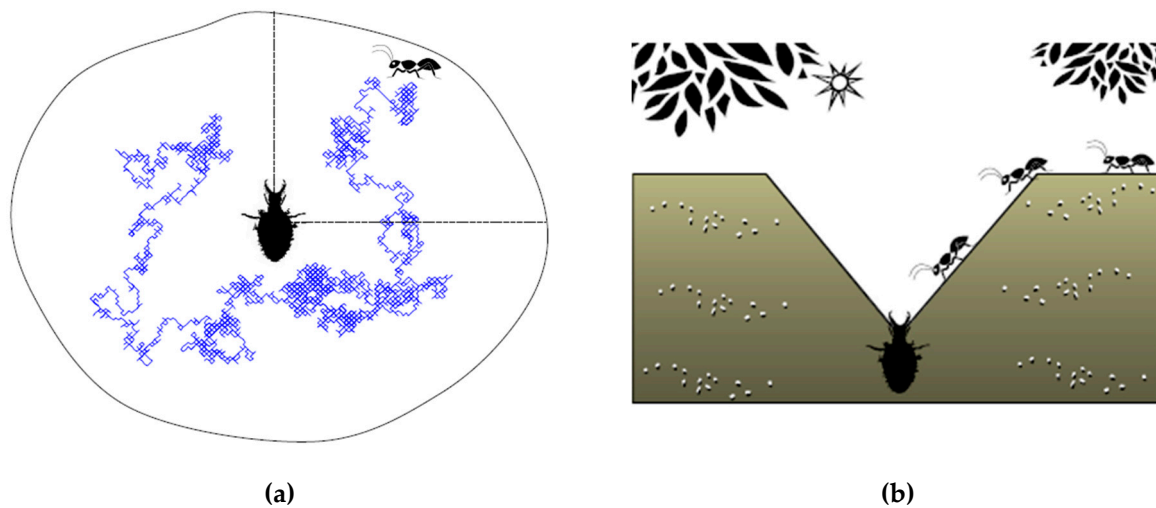


Figure 3. (a) Random walk of the prey inside the trap, and (b) hunting behavior of ant lions (after [33]).

In the ALO algorithm, it is assumed that each prey is trapped by one hunter. Since the goodness of the prey contributes to the ant lion hunting capability, a so-called function “roulette wheel selection (RWS)” is executed here. With this work, the ants with higher fitness have more chance to catch better prey. Considering I as a factor which depends on the ratio of the current repetition and the number of repetitions. The prey sliding in the trap (Figure 3b) is mathematically expressed by below equations. Applying this decrease in the search space helps to achieve a more proper convergence toward optimization.

$$c^t = c^t / I \tag{8}$$

$$d^t = d^t / I \tag{9}$$

Eventually, catching the prey, as well as ant lion reposition, are defined as follows:

$$f(Ant_i^t) < f(Antlion_j^t) \rightarrow Antlion_j^t = Ant_i^t \tag{10}$$

The elite ant lion is then determined, and the position of all relations in the search space is assumed to be affected by the position of the elite member. Let R_A^t be a random walk of the prey near ant lion selected through the RWS, and also R_E^t be the random walk of the same prey near the best hunter, then this process is expressed as follows [33]:

$$Ant_i^t = \frac{R_A^t + R_E^t}{2} \tag{11}$$

2.2. Benchmark Models

As explained earlier, two recently-developed metaheuristic algorithms of biogeography-based optimization (BBO) [35] and the grasshopper optimization algorithm (GOA) [36] are considered as benchmark models for evaluating the results of the proposed ALO technique. The BBO and GOA are nature-inspired algorithms which respectively mimic the biogeography knowledge (i.e., the distribution of different species) and herding behavior of grasshoppers to achieve the optimal solutions of a mathematically defined problem. As a common trait, both methods draw on two major steps, namely migration and mutation in the BBO and exploration and exploitation in the GOA [37,38]. As the first action, some individuals (i.e., the initial population) are generated randomly which represent possible solutions to the problem. During the next steps, the algorithms try to improve the goodness of them by taking special policies. In combination with the ANN [39], these algorithms

aim to overcome the drawbacks of back-propagation technique, like local minima, by suggesting solutions for adjusting the weights and biases. More details about the BBO and GOA are presented in [40–42] and [36,43], respectively.

3. Data Collection and Statistical Analysis

The used database is created by measuring the slump of 103 concrete specimens based on a research by Yeh [2]. Seven slump influential factors, cement (C), slag (S), water (W), fly ash (F), superplasticizer (SP), fine aggregate (FA), and coarse aggregate (CA) are considered as input variables, while the slump is taken to be the output of the predictive models. According to reference paper, the standards of American society or testing and materials (ASTM) was considered for creating concrete specimens. Meanwhile, the conventional slump test (ASTM C143/C143M-00) [44] was used to determine the consistence of fresh concrete. More details about data provision and carried out tests are presented in References [2,45].

Considering the famous ratio of 80:20, the dataset was divided into the training (composed of 82 concrete slump tests) and testing (composed of 21 concrete slump tests) phases. The results of the statistical analyses (i.e., the values of minimum, maximum, mean, and standard deviation) of these factors are presented in Table 1. Moreover, Figure 4a–g show the graphical relationship between the slump and each effective factor.

Table 1. Statistical analyses of the used dataset.

	Slump (cm)	Cement (kg/m ³)	Slag (kg/m ³)	Water (kg/m ³)	Fly ash (kg/m ³)	SP (kg/m ³)	FA (kg/m ³)	CA (kg/m ³)
Minimum	0.0	137.0	0.0	160.0	0.0	4.4	640.6	708.0
Maximum	29.0	374.0	260.0	240.0	193.0	19.0	902.0	1049.9
Mean	18.0	229.9	149.0	197.2	78.0	8.5	739.6	884.0
Standard deviation	8.7	78.9	85.4	20.2	60.5	2.8	63.3	88.4

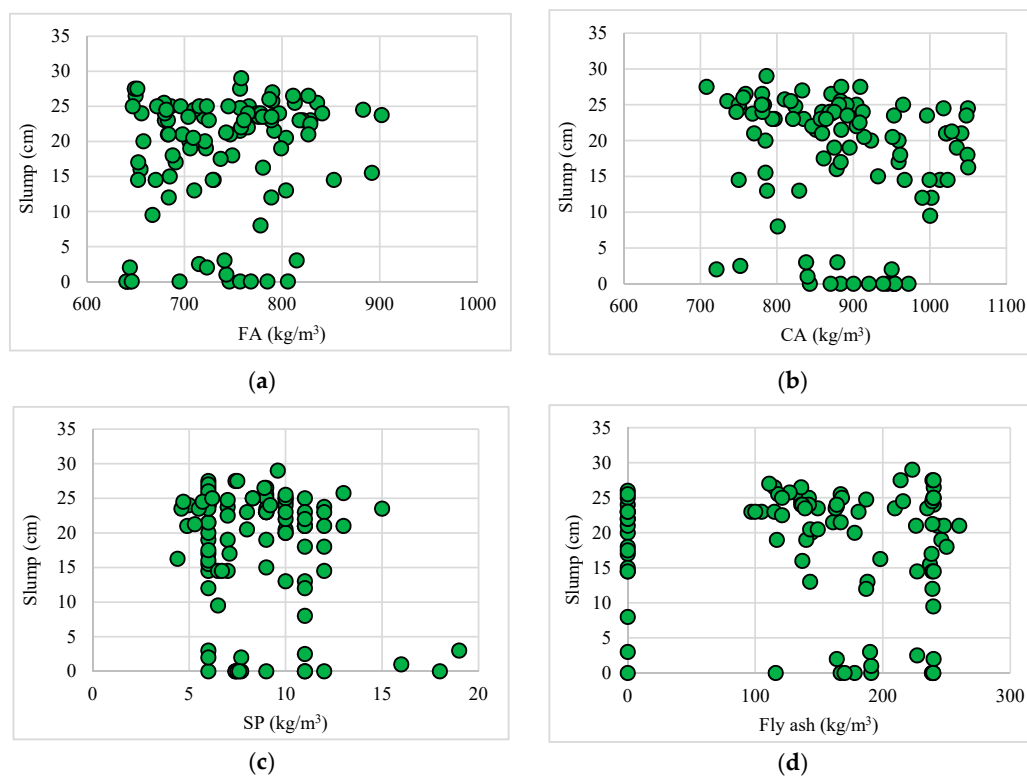


Figure 4. Cont.

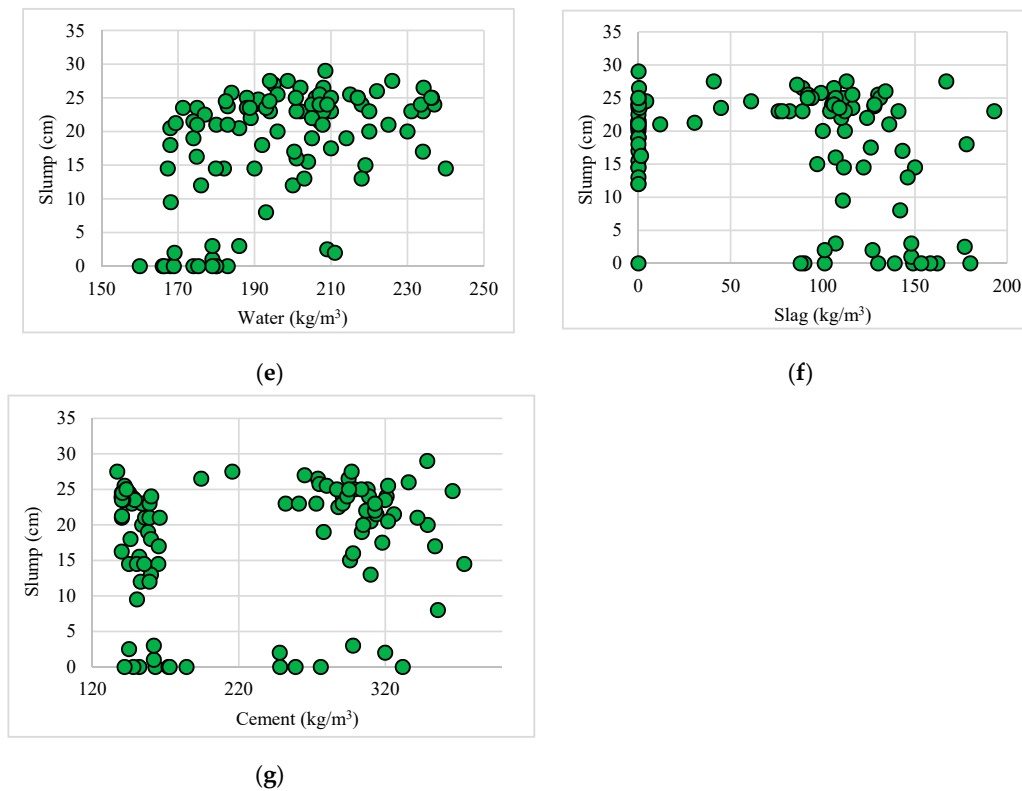


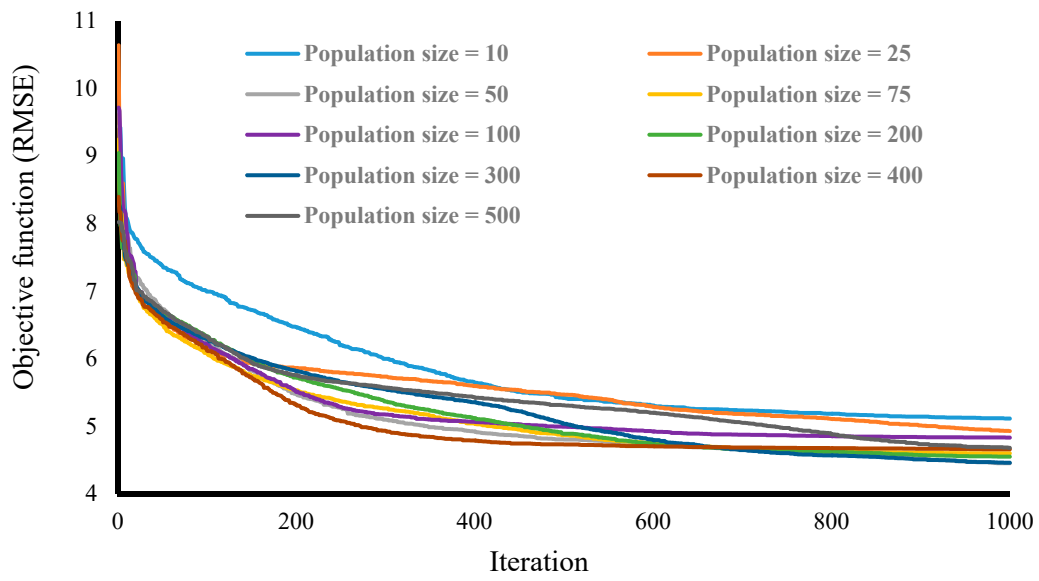
Figure 4. The graphical description of the concrete slump influential factors. (a) FA (kg/m^3), (b) CA (kg/m^3), (c) SP (kg/m^3), (d) Fly ash (kg/m^3), (e) Water (kg/m^3), (f) Slag (kg/m^3), (g) Cement (kg/m^3).

4. Results and Discussion

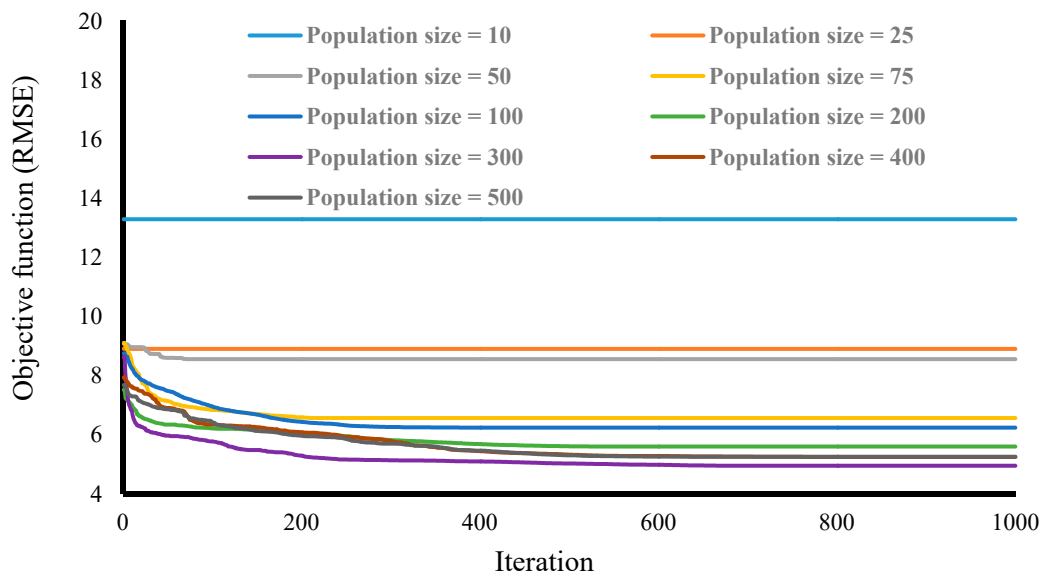
Evaluating the efficiency of the ant lion optimization technique for predicting concrete slump is the pivotal objective of this paper. To fulfil this purpose, the ALO algorithm is coupled with a multi-layer perceptron neural network to fine-tune its parameters. The performance of BBO and GOA optimization techniques was also investigated as benchmark models. In the first stage, based on the number of neurons, a trial and error process was carried out to determine the most suitable NN structure. In this regard, the MLP with 6 nodes in its unique hidden layer produced the most consistent results. Therefore, this structure was considered as the basic NN for being combined with the optimization techniques. In the following, the mathematical equation of the MLP is given to the ALO, BBO, and GOA as the problem function. The optimization process is detailed in the below section.

4.1. ALO, BBO, and GOA Conventional Methods for Optimizing the NN

When it comes to hybrid optimization techniques, population size is considered an influential parameter which highly affects the performance of the proposed algorithm. In fact, this value indicates the number of the individuals in the society (e.g., the number of ant lions in the ALO technique). Each network was tested by nine different population sizes (i.e., 10, 25, 50, 75, 100, 200, 300, 400, and 500) [46]. The RMSE was defined as the objective function to measure the error of the performance at the end of each iteration. Each model performed within 1000 repetitions to optimize the neural parameters (i.e., connecting weights and biases) of the proposed NN. More clearly, at each iteration, the found solution contained the mentioned parameters. The NN was reconstructed by means of the obtained parameters and performed to estimate slump. Then, the RMSE between the targets and outputs was measured as the objective function. The result was a convergence curve showing the decrease of the error. Figure 5a–c shows the obtained convergence curves of the implemented BBO-NN, GOA-NN, and ALO-NN ensembles, respectively.

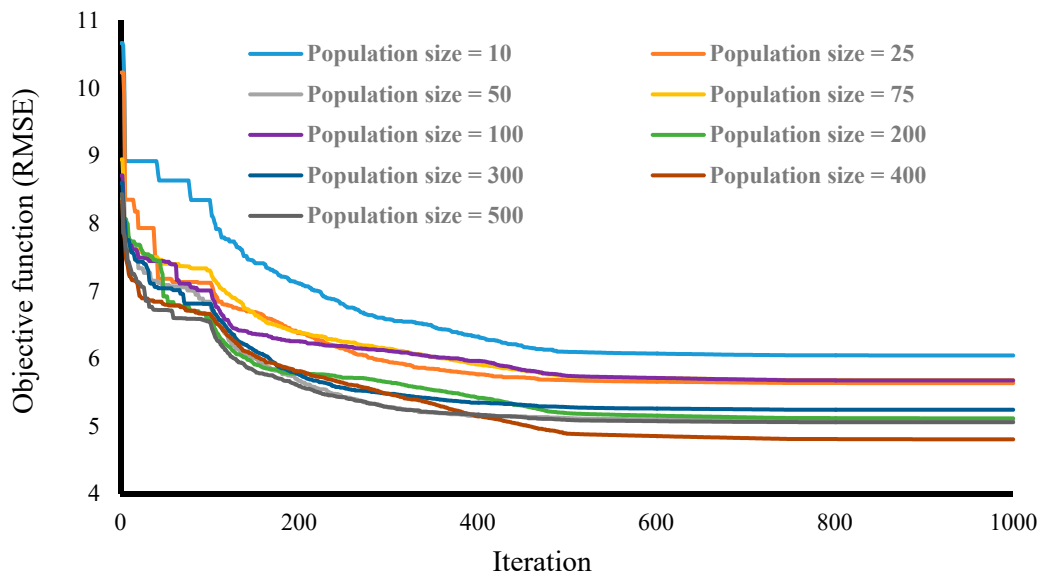


(a) BBO-NN



(b) GOA-NN

Figure 5. Cont.



(c) ALO-NN

Figure 5. The sensitivity analysis based on the model complexity for the (a) BBO-NN, (b) GOA-NN, and (c) ALO-NN.

As is illustrated, all three models decreased the majority of the RMSE within the first 600 iterations. For better illustration, Figure 6 denotes the best response of the tested networks in terms of the RMSE. Accordingly, the ALO, BBO, and GOA with population sizes of 400, 50, and 300 performed more efficiently than other versions. It is also seen that the overall behavior of the RMSE is downward for GOA-NN, while it fluctuates for the two other algorithms. The proposed ALO-NN achieved the RMSE of 4.955 at the 678th try, and remained steady thereafter. As for the BBO and GOA, the RMSE was obtained 4.4508 and 4.9552, respectively. Notably, the implementation time (for all 1000 repetitions) were obtained 32,784.89, 645.38, and 4273.3 seconds on an operating system at 2.5 GHz and 6 Gigabytes of RAM.

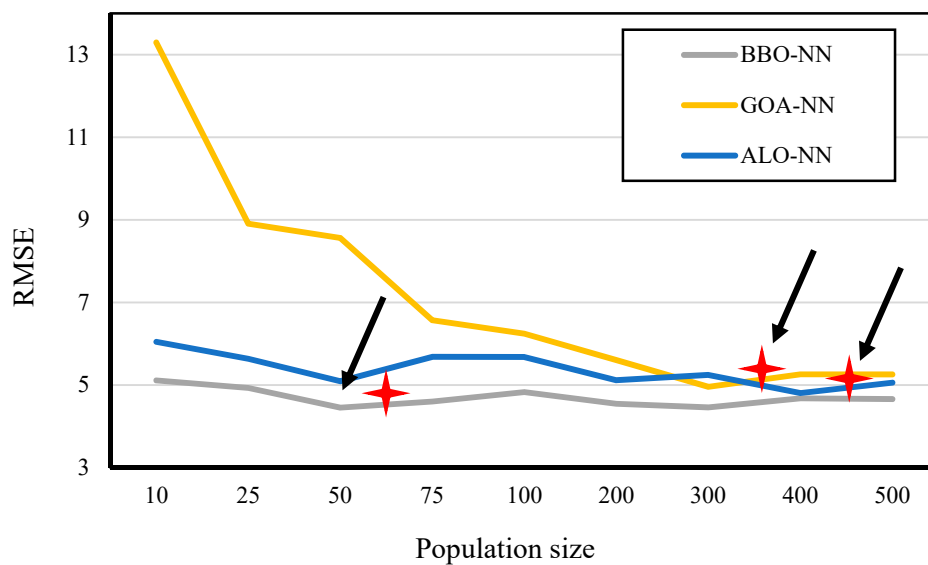


Figure 6. The final root mean square error (RMSE) values versus the population size.

4.2. Performance Evaluation and Discussion

After determining the best-fitted structures of the ALO-NN, BBO-NN, and GOA-NN, their responses were evaluated to measure the accuracy of the models. To this end, the RMSE and MAE were calculated. Figures 7 and 8 depict the graphical comparisons between the actual and predicted slumps in the training and testing phases, respectively. The error values (i.e., the difference between the target and outputs) are also depicted in these figures.

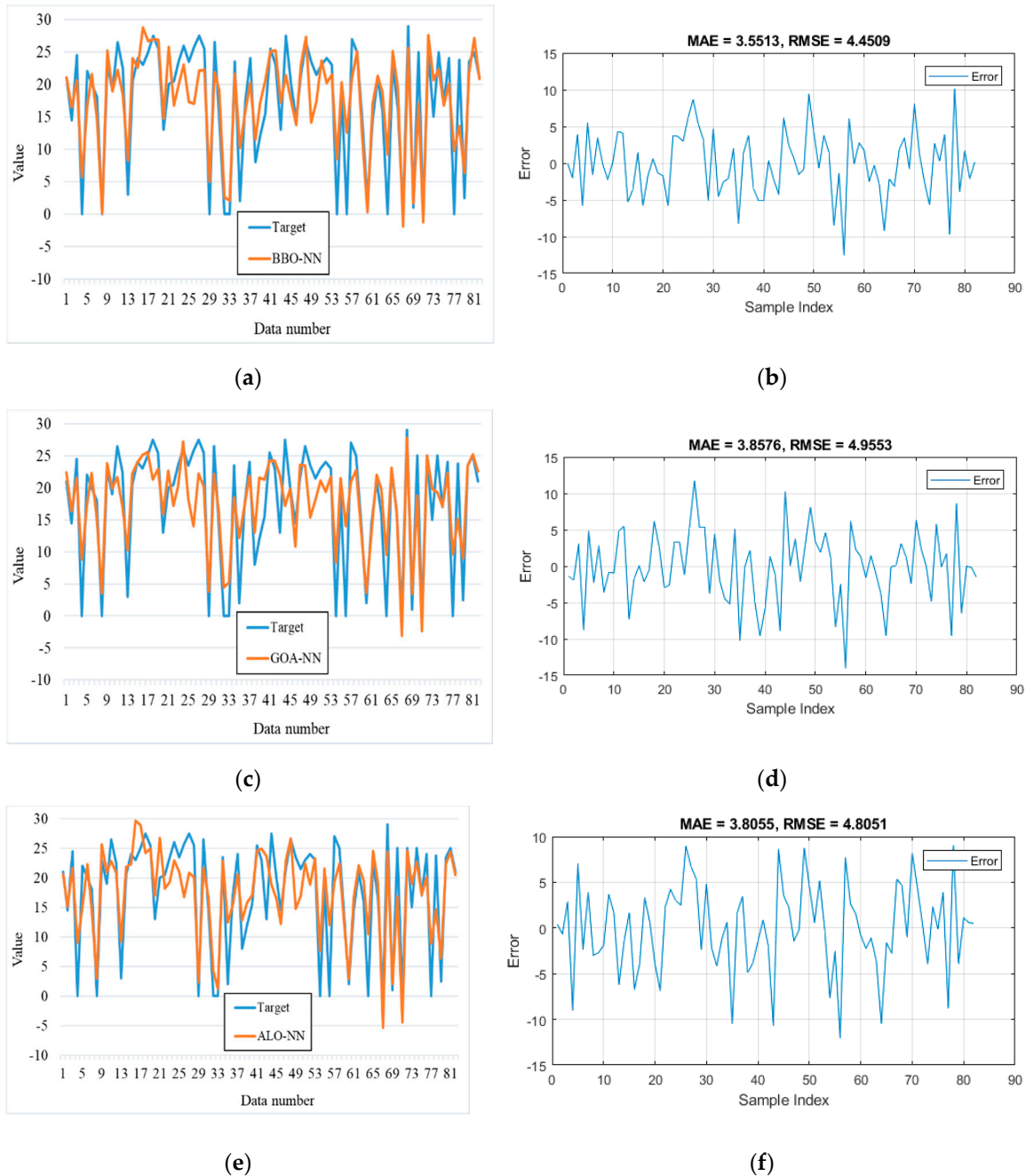
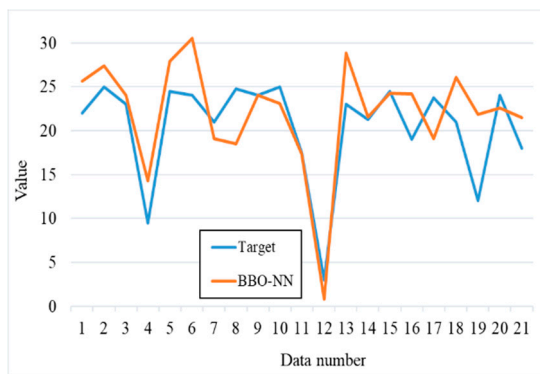
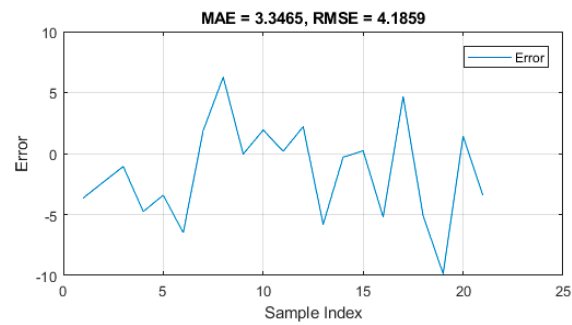


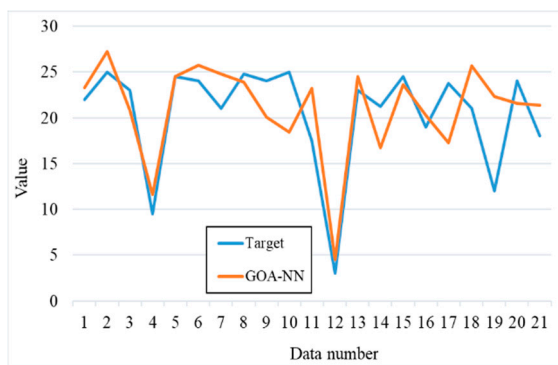
Figure 7. The training results obtained for (a,b) BBO-NN, (c,d) GOA-NN, and (e,f) ALO-NN predictions.



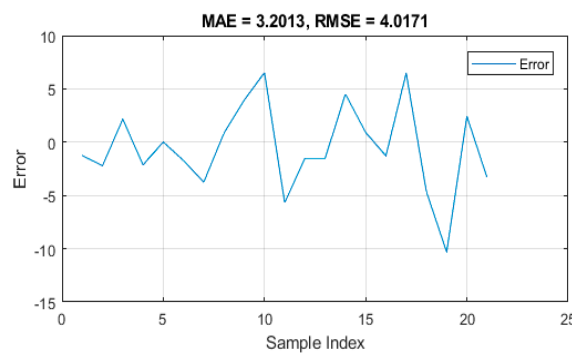
(a)



(b)



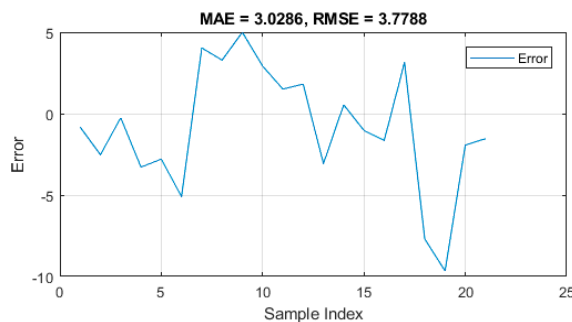
(c)



(d)



(e)



(f)

Figure 8. The testing results obtained for (a,b) BBO-NN, (c,d) GOA-NN, and (e,f) ALO-NN predictions.

The calculated RMSEs for the training samples (4.4509, 4.9553, and 4.8051, respectively, for the BBO-NN, GOA-NN, and ALO-NN) indicate that the computational parameters suggested by all three metaheuristic algorithms develop an MLP with an acceptable accuracy. This claim can also be supported by the training MAEs (3.5513, 3.8576, and 3.8055). From a comparison viewpoint, regarding the lower error values, the BBO acquired a better understanding of the relationship between slump and its effective factors, compared to the two other networks. Moreover, the ALO outperformed GOA in this phase.

As for the testing phase, the computed RMSEs (4.1859, 4.0171, and 3.7788) showed disagreement between the learning and generalization power of the used ensembles. In this sense, despite the higher accuracy of the BBO in the training phase, the ALO produced more consistent results for concretes with unseen conditions. Furthermore, GOA performed more efficiently than BBO in the testing stage.

In addition to RMSE, the obtained MAEs (3.3465, 3.2013, and 3.0286) revealed that the ALO was the most effective evolutionary algorithm for optimizing MLP, followed by GOA and BBO.

Overall, it was concluded that, although the BBO trained the ANN more effectively than the two other techniques, the ALO was found to have the highest generalization capability. However, investigating the reason for this requires further analysis and expert coding knowledge; one possible reason could be the greater number of steps taken by ALO to achieve the target, because it is an obvious distinction between the mechanisms of the mentioned techniques. As explained, six major steps are needed to implement the ALO, whilst both BBO and GOA execute the optimization with two steps.

Focusing on the range of the products, there are some negative values in the training data. In details, the actual slump values in the training phase vary from 0 to 29 cm, while the predicted values by the BBO-NN, GOA-NN, and ALO-NN range in, [-1.922, 28.761], [-3.113, 27.742], and [-5.346, 29.722], respectively. Needless to say, negative slump values do not indicate any physical meaning. The authors believe that the reason for this can be sought in the wide range of actual slumps (sample variance = 76.57). The distribution of input data might be another misleading parameter. Referring to Figure 4d–f, for instance, it can be seen that there is a considerable number of concrete specimens which did not show any sensitivity to the changes in the amount of slag and fly ash (slump equals 0 for these data). However, it should be noted that the slump is a function of all input parameters.

In comparison with some of previous studies which have used the same dataset to train their intelligent approaches, or same statistical indexes to assess their model performance [47–52], the result of our study are more promising. Yeh [24], for example, found that the ANN with an RMSE of 4.12 cm is a capable tool for simulating the slump. Likewise, Yeh [25] and Yeh [2] achieved the RMSEs of 4.03 and 8.51 by employing ANN in their research. This is because the RMSE of the elite model of the current study was less than 4 cm (i.e., 3.7788 cm) obtained by the proposed ALO-NN ensemble. Another item which could be pointed out is the enhancement of the ANN performance in incorporation with the ALO optimization algorithm. In other words, the weights and biases suggested by ALO constructed a more capable ANN compared to those suggested through its regular learning model. Noting that the current study was carried out for typical concrete mixture (i.e. used Portland cement), and it is found that the employed metaheuristic sciences have excellent performance and potential to predict the slump simulation of special concrete like self-compacting concrete (SCC) [47], high strength concrete (HSC) [23], and so on. Testing the used networks for the mentioned aims could be an appropriate idea for future studies.

Moreover, according to Yeh [25], the American Concrete Pavement Association (ACPA) [53] has considered that measured differences in slumps of lower than 2 inches (5.08 cm) are typical for sampling, testing, and material variation. Therefore, the prediction error of the all three implemented models, and especially the ALO-NN, is relatively low, and lies in an acceptable extent. Hence, the suggested models are potent enough to be properly used in the industry. As difficulties have been associated with laboratory models, and considering the high robustness of soft computing methods in the field of slump modelling, intelligent tools may be accurate and inexpensive alternatives to traditional approaches.

In the last part of this study, a slump predictive formula is presented (Equation (12)). Note that, this formula is developed based on the weights and biases that have been suggested by the most successful neural ensemble (i.e., the ALO-NN). More specifically, this equation indicates the neural relationship established in the unique output neuron of the used MLP network. Therefore, utilizing it entails calculating some middle parameters which are the outputs of the hidden neurons.

$$\text{Slump} = -0.1317 \times Z1 - 0.8109 \times Z2 + 0.5922 \times Z3 + 0.3680 \times Z4 + 0.8241 \times Z5 - 0.5218 \times Z6 - 0.2127 \quad (12)$$

In above formula, $Z1, Z2, \dots, Z6$ are middle parameters and are obtained by Equation (13). This is worth noting that the activation function of the hidden neurons is “Tangent-Sigmoid” (briefly Tansig) which is expressed by Equation (14).

$$\begin{bmatrix} Z1 \\ Z2 \\ Z3 \\ Z4 \\ Z5 \\ Z6 \end{bmatrix} = \text{Tansig} \left(\begin{bmatrix} 0.0384 & -0.7997 & -0.0212 & -0.8032 & 0.8395 & -0.6082 & -0.9534 \\ -0.5088 & 0.7849 & -0.9327 & -0.8099 & 0.5248 & 0.5034 & 0.5838 \\ -0.4529 & -0.2884 & -0.9269 & -1.0198 & 0.7335 & -0.7290 & -0.1157 \\ -0.3728 & -0.9210 & 0.3470 & 0.5572 & 0.7748 & -0.9547 & 0.5835 \\ -0.9642 & 0.3015 & 0.6630 & 0.1027 & -0.1102 & -0.9227 & 0.9675 \\ -0.3548 & -0.0485 & -0.2256 & 1.5514 & 0.0741 & -0.6239 & -0.5380 \end{bmatrix} \begin{bmatrix} C \\ S \\ F \\ W \\ SP \\ CA \\ FA \end{bmatrix} + \begin{bmatrix} -1.8084 \\ 1.0850 \\ 0.3617 \\ -0.3617 \\ -1.0850 \\ -1.8084 \end{bmatrix} \right) \quad (13)$$

$$\text{Tansig} (x) = \frac{2}{1 + e^{-2x}} - 1 \quad (14)$$

5. Conclusions

The applicability of a state-of-the-art metaheuristic technique was investigated for modelling the slump of concrete. The ant lion optimizer was applied to a neural network for fine-tuning the computational parameters contributing to slump effective parameters. In addition, two well-known evolutionary techniques of BBO and GOA were considered as benchmark models. The MLP network with six processor units in the hidden layer was mathematically introduced to the mentioned algorithms to find the most appropriate weights and biases for predicting the slump. The carried-out sensitivity analysis outlined that the ALO, BBO, and GOA with population size 400, 50, and 300 present the best-fitted neural ensemble. The calculated error criteria revealed that the ANN constructed by the BBO understood the relationship between the slump and influential factors better than the two other algorithms, while the ALO surpassed both benchmark models of GOA and BBO in predicting the slump pattern. Meanwhile, regarding the acceptable prediction error (3.3465, 3.2013, and 3.0286, respectively, for the BBO-NN, GOA-NN, and ALO-NN), this study showed that the combination of the ANN and hybrid optimizers can construct robust and inexpensive alternatives to traditional models of slump evaluation. The slump predictive formula of the MLP optimized by the ALO evolutionary technique was also presented.

Author Contributions: First draft written by H.M., Methodology, D.T.B., B.K., H.M. and L.K.F.; data curation, H.M., A.M. and L.K.F.; writing—original draft preparation, B.K. Edited, restructured, and professionally optimized the manuscript.

Funding: The APC was funded by the RIKEN Center for Advanced Intelligence > Project (AIP), Japan.

Conflicts of Interest: The authors declare no conflict of interest.

References

1. Henigal, A.; Elbeltgai, E.; Eldwiny, M.; Serry, M. Artificial Neural Network Model for Forecasting Concrete Compressive Strength And Slump In Egypt. *J. Al Azhar Univ. Eng. Sect.* **2016**, *11*, 435–446. [CrossRef]
2. Yeh, I.-C. Modeling slump flow of concrete using second-order regressions and artificial neural networks. *Cem. Concr. Compos.* **2007**, *29*, 474–480. [CrossRef]
3. Antiohos, S.; Papadakis, V.; Tsimas, S. Rice husk ash (RHA) effectiveness in cement and concrete as a function of reactive silica and fineness. *Cem. Concr. Res.* **2014**, *61*, 20–27. [CrossRef]
4. McCulloch, W.S.; Pitts, W. A logical calculus of the ideas immanent in nervous activity. *Bull. Math. Biophys.* **1943**, *5*, 115–133. [CrossRef]
5. Moayedi, H.; Abdullahi, M.a.M.; Nguyen, H.; Rashid, A.S.A. Comparison of dragonfly algorithm and Harris hawks optimization evolutionary data mining techniques for the assessment of bearing capacity of footings over two-layer foundation soils. *Eng. Comput.* **2019**, 1–11. [CrossRef]
6. Moayedi, H.; Armaghani, D.J. Optimizing an ANN model with ICA for estimating bearing capacity of driven pile in cohesionless soil. *Eng. Comput.* **2017**, 1–10. [CrossRef]
7. Moayedi, H.; Foong, L.K.; Nguyen, H.; Bui, D.T.; Jusoh, W.A.W.; Rashid, A.S.A. Optimizing ANN models with PSO for predicting in short building seismic response. *Eng. Comput.* **2019**, 1–16. [CrossRef]
8. Moayedi, H.; Mehdi, R.; Abolhasan, S.; Wan, A.W.J.; Safuan, A.R.A. Optimization of ANFIS with GA and PSO estimating α in driven shafts. *Eng. Comput.* **2019**, *35*, 1–12. [CrossRef]

9. ASCE Task Committee. Artificial neural networks in hydrology. II: Hydrologic applications. *J. Hydrol. Eng.* **2000**, *5*, 124–137. [[CrossRef](#)]
10. Moayedi, H.; Hayati, S. Modelling and optimization of ultimate bearing capacity of strip footing near a slope by soft computing methods. *Appl. Soft Comput.* **2018**, *66*, 208–219. [[CrossRef](#)]
11. Moayedi, H.; Huat, B.B.; Mohammad Ali, T.A.; Asadi, A.; Moayedi, F.; Mokhberi, M. Preventing landslides in times of rainfall: Case study and FEM analyses. *Disaster Prev. Manag.* **2011**, *20*, 115–124. [[CrossRef](#)]
12. Moayedi, H.; Hayati, S. Applicability of a CPT-Based Neural Network Solution in Predicting Load-Settlement Responses of Bored Pile. *Int. J. Geomech.* **2018**, *18*, 06018009. [[CrossRef](#)]
13. Seyedashraf, O.; Mehrabi, M.; Akhtari, A.A. Novel approach for dam break flow modeling using computational intelligence. *J. Hydrol.* **2018**, *559*, 1028–1038. [[CrossRef](#)]
14. Hecht-Nielsen, R. Theory of the backpropagation neural network. In *Neural Networks for Perception*; International 1989 Joint Conference on Neural Networks; IEEE: Washington, DC, USA, 1989; pp. 65–93. [[CrossRef](#)]
15. Moayedi, H.; Moatamediyani, A.; Nguyen, H.; Bui, X.-N.; Bui, D.T.; Rashid, A.S.A. Prediction of ultimate bearing capacity through various novel evolutionary and neural network models. *Eng. Comput.* **2019**, *35*. [[CrossRef](#)]
16. Moayedi, H.; Mosallanezhad, M.; Mehrabi, M.; Safuan, A.R.A.; Biswajeet, P. Modification of landslide susceptibility mapping using optimized PSO-ANN technique. *Eng. Comput.* **2019**, *35*, 967–984. [[CrossRef](#)]
17. Aksoy, H.S.; Gör, M.; İnal, E. A new design chart for estimating friction angle between soil and pile materials. *Geomechanics and Engineering* **2016**, *10*, 315–324. [[CrossRef](#)]
18. Nguyen, H.; Moayedi, H.; Sharifi, A.; Amizah, W.J.W.; Safuan, A.R.A. Proposing a novel predictive technique using M5Rules-PSO model estimating cooling load in energy-efficient building system. *Eng. Comput.* **2019**, *35*, 1–11. [[CrossRef](#)]
19. Vakhshouri, B.; Nejadi, S. Prediction of compressive strength of self-compacting concrete by ANFIS models. *Neurocomputing* **2018**, *280*, 13–22. [[CrossRef](#)]
20. Bilgehan, M.; Kurtoglu, A.E. ANFIS-based prediction of moment capacity of reinforced concrete slabs exposed to fire. *Neural Comput. Appl.* **2016**, *27*, 869–881. [[CrossRef](#)]
21. Juncai, X.; Qingwen, R.; Zhenzhong, S. Prediction of the strength of concrete radiation shielding based on LS-SVM. *Ann. Nucl. Energy* **2015**, *85*, 296–300. [[CrossRef](#)]
22. Li, X.; Yi, G.; Wang, W.; Sun, J.; Li, Y. *Research and Application of RBF Neural Network-Based Osmotic Pressure Forecast Model for Concrete-Faced Rockfill Dam*; IOP Publishing: Bristol, UK, 2018; Volume 198. [[CrossRef](#)]
23. Oztas, A.; Pala, M.; Ozbay Ea Kanca, E.; Caglar, N.; Bhatti, M.A. Predicting the compressive strength and slump of high strength concrete using neural network. *Constr. Build. Mater.* **2006**, *20*, 769–775. [[CrossRef](#)]
24. Yeh, I.-C. Simulation of concrete slump using neural networks. *Constr. Mater.* **2009**, *162*, 11–18. [[CrossRef](#)]
25. Yeh, I.-C. Exploring concrete slump model using artificial neural networks. *J. Comput. Civ. Eng.* **2006**, *20*, 217–221. [[CrossRef](#)]
26. Gao, W.; Raftari, M.; Rashid, A.S.A.; Mu'azu, M.A.; Jusoh, W.A.W. A predictive model based on an optimized ANN combined with ICA for predicting the stability of slopes. *Eng. Comput.* **2019**, 1–20. [[CrossRef](#)]
27. Bui, D.T.; Moayedi, H.; Gör, M.; Jaafari, A.; Foong, L.K. Predicting slope stability failure through machine learning paradigms. *ISPRS Int. Geo-Inf.* **2019**, *8*, 395. [[CrossRef](#)]
28. Yuan, C.; Moayedi, H. The performance of six neural-evolutionary classification techniques combined with multi-layer perception in two-layered cohesive slope stability analysis and failure recognition. *Eng. Comput.* **2019**, 1–10. [[CrossRef](#)]
29. Nguyen, H.; Mehrabi, M.; Kalantar, B.; Moayedi, H.; Abdullahi, M.A.M. Potential of hybrid evolutionary approaches for assessment of geo-hazard landslide susceptibility mapping. *Geomat. Nat. Hazards Risk* **2019**, *10*, 1667–1693. [[CrossRef](#)]
30. Xu, J.; Shen, Z.; Ren, Q.; Xie, X.; Yang, Z. Geometric Semantic Genetic Programming Algorithm and Slump Prediction. *arXiv* **2017**, arXiv:1709.06114.
31. Chandwani, V.; Agrawal, V.; Nagar, R. Modeling slump of ready mix concrete using genetic algorithms assisted training of Artificial Neural Networks. *Expert Syst. Appl.* **2015**, *42*, 885–893. [[CrossRef](#)]
32. Chen, L.; Kou, C.-H.; Ma, S.-W. Prediction of slump flow of high-performance concrete via parallel hyper-cubic gene-expression programming. *Eng. Appl. Artif. Intell.* **2014**, *34*, 66–74. [[CrossRef](#)]
33. Mirjalili, S. The ant lion optimizer. *Adv. Eng. Softw.* **2015**, *83*, 80–98. [[CrossRef](#)]

34. Spoljaric, T.; Pavic, I. Performance analysis of an ant lion optimizer in tuning generators' excitation controls in multi machine power system. In Proceedings of the 2018, 41st International Convention on Information and Communication Technology, Electronics and Microelectronics (MIPRO), Opatija, Croatia, 21–25 May 2018.
35. Simon, D. Biogeography-based optimization. *IEEE Trans. Evolut. Comput.* **2008**, *12*, 702–713. [CrossRef]
36. Saremi, S.; Mirjalili, S.; Lewis, A. Grasshopper optimisation algorithm: Theory and application. *Adv. Eng. Softw.* **2017**, *105*, 30–47. [CrossRef]
37. Moayedi, H.; Bui, D.T.; Gör, M.; Pradhan, B.; Jaafari, A. The feasibility of three prediction techniques of the artificial neural network, adaptive neuro-fuzzy inference system, and hybrid particle swarm optimization for assessing the safety factor of cohesive slopes. *ISPRS Int. Geo-Inf.* **2019**, *8*, 391. [CrossRef]
38. Yuan, C.; Moayedi, H. Evaluation and comparison of the advanced metaheuristic and conventional machine learning methods for prediction of landslide occurrence. *Eng. Comput.* **2019**, *36*. [CrossRef]
39. Mirjalili, S.; Mirjalili, S.M.; Lewis, A. Let a biogeography-based optimizer train your multi-layer perceptron. *Inf. Sci.* **2014**, *269*, 188–209. [CrossRef]
40. Ma, H.; Simon, D. Blended biogeography-based optimization for constrained optimization. *Eng. Appl. Artif. Intell.* **2011**, *24*, 517–525. [CrossRef]
41. Simon, D. A probabilistic analysis of a simplified biogeography-based optimization algorithm. *Evolut. Comput.* **2011**, *19*, 167–188. [CrossRef]
42. Ma, H.; Simon, D. Analysis of migration models of biogeography-based optimization using Markov theory. *Eng. Appl. Artif. Intell.* **2011**, *24*, 1052–1060. [CrossRef]
43. Mirjalili, S.Z.; Mirjalili, S.; Saremi, S.; Faris, H.; Aljarah, I. Grasshopper optimization algorithm for multi-objective optimization problems. *Appl. Intell.* **2018**, *48*, 805–820. [CrossRef]
44. ASTM C 143. *Standard Test Method for Slump of Hydraulic-Cement Concrete*; ASTM International: West Conshohocken, PA, USA, 2005.
45. Yeh, I.-C.; Chen, J.W. Modeling Workability of Concrete Using Design of Experiments and Artificial Neural Networks. *J. Technol.* **2005**, *20*, 153–162.
46. Bui, D.T.; Abdullahi, M.a.M.; Ghareh, S.; Moayedi, H.; Nguyen, H. Fine-tuning of neural computing using whale optimization algorithm for predicting compressive strength of concrete. *Eng. Comput.* **2019**, *1–12*. [CrossRef]
47. Nehdi, M.; El Chabib, H.; El Naggat, M.H. Predicting performance of self-compacting concrete mixtures using artificial neural networks. *Mater. J.* **2001**, *98*, 394–401.
48. Gao, W.; Wang, W.; Dimitrov, D.; Wang, Y. Nano properties analysis via fourth multiplicative ABC indicator calculating. *Arabian journal of chemistry* **2018**, *11*, 793–801. [CrossRef]
49. Gao, W.; Dimitrov, D.; Abdo, H. Tight independent set neighborhood union condition for fractional critical deleted graphs and ID deleted graphs. *Discrete & Continuous Dynamical Systems-S* **2018**, *12*, 711–721.
50. Gao, W.; Guirao, J.L.G.; Abdel-Aty, M.; Xi, W. An independent set degree condition for fractional critical deleted graphs. *Discrete & Continuous Dynamical Systems-S* **2019**, *12*, 877–886.
51. Gao, W.; Guirao, J.L.G.; Basavanagoud, B.; Wu, J. Partial multi-dividing ontology learning algorithm. *Inf. Sci.* **2018**, *467*, 35–58. [CrossRef]
52. Gao, W.; Wu, H.; Siddiqui, M.K.; Baig, A.Q. Study of biological networks using graph theory. *Saudi J. Biol. Sci.* **2018**, *25*, 1212–1219. [CrossRef]
53. ACPAAW. Available online: <http://www.pavement.com/PavTech/Tech/FATQ/fatqslump.html> (accessed on 1 May 2005).

